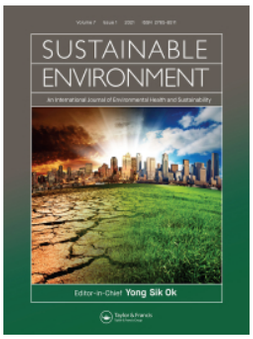

Taylor & Francis
Taylor & Francis Group

Sustainable Environment

An international journal of environmental health and sustainability

ISSN: (Print) (Online) Journal homepage: www.tandfonline.com/journals/oaes21

# Synthesis of magnesium oxide from waste magnesium-rich *Cucurbita pepo* (pumpkin) seeds

**Patience Oduroa Agyapong, Emmanuel Gikunoo, Emmanuel Kwesi Arthur, Daniel Adjah Anang, Frank Ofori Agyemang, Gordon Foli & Douglas Siaw Baah |**

**To cite this article:** Patience Oduroa Agyapong, Emmanuel Gikunoo, Emmanuel Kwesi Arthur, Daniel Adjah Anang, Frank Ofori Agyemang, Gordon Foli & Douglas Siaw Baah | (2023) Synthesis of magnesium oxide from waste magnesium-rich *Cucurbita pepo* (pumpkin) seeds, Sustainable Environment, 9:1, 2258473, DOI: 10.1080/27658511.2023.2258473

**To link to this article:** https://doi.org/10.1080/27658511.2023.2258473



Published online: 21 Sep 2023.

SUSTAINABLE ENVIRONMENT
2023, VOL. 9, NO. 1, 2258473
https://doi.org/10.1080/27658511.2023.2258473

Taylor & Francis
Taylor & Francis Group

ENVIRONMENTAL RESOURCE MANAGEMENT | RESEARCH ARTICLE

OPEN ACCESS Check for updates

# Synthesis of magnesium oxide from waste magnesium-rich *Cucurbita pepo* (pumpkin) seeds

Patience Oduroa Agyapong[a,b], Emmanuel Gikunoo[a], Emmanuel Kwesi Arthur[a], Daniel Adjah Anang[c], Frank Ofori Agyemang[a], Gordon Foli[d] and Douglas Siaw Baah[e]

[a]Materials Engineering Department, Kwame Nkrumah University of Science and Technology, Kumasi, Ghana; [b]Grading and Inspection Department, Timber Industry Development Division, Techiman, Ghana; [c]Chemical Engineering Department, Kwame Nkrumah University of Science and Technology, Kumasi, Ghana; [d]Geological Engineering Department, Kwame Nkrumah University of Science and Technology, Kumasi, Ghana; [e]Forestry Research Institute of Ghana, Council for Scientific and Industrial Research, Kumasi, Ghana

**ABSTRACT**

Recent studies have focused on the processing of biowaste to obtain added value and to reduce organic waste in the general stream. This study investigated the synthesis of magnesium oxide (MgO) from magnesium-rich *Cucurbita pepo* (pumpkin) seeds for a precursor solution as a reducing agent via an eco-friendly method for the first time. The pumpkin seeds were ashed at 550°C for 6 h and subjected to acid-leaching. $Mg(OH)_2$ was then precipitated using an aqueous solution of 2.0 M NaOH. The $Mg(OH)_2$ was then calcined at 550°C for 4 h to obtain MgO. Physicochemical properties (i.e. proximate analysis, elemental composition, electrical conductivity (EC), pH) and selected heavy metals (i.e. Pb, Fe, As, Cd, Cr, Hg, Cu, and Ni) analyses were conducted on the seed samples and as-synthesized MgO. X-ray fluorescence (XRF), X-ray diffraction (XRD), Fourier-transform infrared (FTIR), citric acid test (CAT), and acid neutralization capacity (ANC) tests were techniques used to characterize the synthesized MgO. The results revealed the percentage yield of the MgO to be 23%. The pH of the as-synthesized MgO was recorded as 10.63. XRF studies showed that MgO made up 75.1% of the total weight synthesized. XRD results showed the presence of crystalline cubic structures of MgO. FTIR results showed a peak at 584 $cm^{-1}$ which confirmed the formation of MgO. The produced MgO was highly reactive, with a CAT time of 2 s. The ANC of the MgO was high at 22.77 $mol^{+}/kg$. Also, metal concentrations such as Fe, Cu, Cd, Ni, Pb, Hg, As, and Cr in MgO were below the WHO stipulated limits of 350, 36, 0.8, 35, 85, 0.03, 40, and 100, respectively. This implies its suitability for soil remediation purposes. Results indicate that the as-synthesized MgO from *Cucurbita pepo* (*C. pepo*) seeds could be used for several applications due to its high alkalinity, reactivity, and fast CAT time.

**ARTICLE HISTORY**
Received 26 February 2023
Accepted 07 September 2023

**KEYWORDS**
magnesium oxide; *Cucurbita pepo* seeds; biowaste; biosynthesis; environmental resources management

## 1. Introduction

The rise in the development of new technologies is creating opportunities for the use of new, innovative, and waste materials. These materials can be tailored to possess the right mix of microstructure and properties for innovative solutions to societal problems. Several materials including metal oxides have been reported in the literature to possess unique functionalities and applications in numerous fields (Dehghan et al., 2022; Kalita et al., 2021; Mohamed et al., 2021; THI Tran et al., 2021). One of these metals, magnesium (Mg) and its compounds, since early 2000 has found extensive application within the healthcare industry (DE Baaij et al., 2015; Safford et al., 2015; Witte, 2010). As a result, the use of Mg and its compounds has risen requiring an increase in its production (Hornak, 2021; Nagappa & Chandrappa, 2007). Magnesium oxide (MgO) is one of the most important inorganic oxides in waste and toxicity management (FOUDA et al., 2021).

MgO use is progressively gaining attention in almost every application. Research proceedings have published its outstanding use of paints (Gysau, 2006), in hazardous waste remediation (GARCIA et al., 2004; GIRO-Paloma et al., 2020; Nagappa & Chandrappa, 2007; Shen et al., 2018, 2019), as catalyst and catalyst support material (Julkapli & Bagheri, 2016). Other applications of MgO include refractory and battery material (Zhai et al., 2019), wastewater remediation (Jamil et al., 2015), agricultural activities (Hornak, 2021), photocatalysis (Amina et al., 2020), toxic gas adsorbents (Camtakan et al., 2012; FERNANDES et al., 2020) and many vital applications (Ahmed & ABOU-GAMRA, 2016). The medicinal importance of MgO can also not

**CONTACT** Emmanuel Gikunoo egikunoo.soe@knust.edu.gh Materials Engineering Department, Kwame Nkrumah University of Science and Technology, Kumasi, Ghana

**Reviewing editor:** Michelle Bloor Scotland's Rural College, School of earth and environmental science, United Kingdom

be ignored (Guerrera et al., 2009; Sawai et al., 2000). Its increasing use as an antacid and laxative and hence over-the-counter medication has also drastically increased its demand (Mori et al., 2021).

MgO is notably obtained from their orebodies (magnesite, dolomite, brucite and olivine) (Shand, 2006) and seawater or brine (HØY-Petersen & Rizley, 2020; Zhang et al., 2021). There is, however, no universal access to these resources, as they tend to be concentrated only in some areas of the world (Daigle & DeCarlo, 2022). Whereas the orebodies are mainly concentrated in a few countries in Asia, Europe, North and South America (Wu et al., 2021), seawater/brine is not accessible to land-locked areas, hence other sources of MgO production are necessary to supplement the high demand of MgO being predicted. Again, research has shown that the low concentration of magnesium in seawater (~1.3 g/cm$^3$) gives rise to design problems during its synthesis (Kulekci, 2008; Song & Atrens, 1999). Also, the extraction of MgO from their raw materials has been reported to negatively influence their environment (HØY-Petersen & Rizley, 2020; Zhang et al., 2021). Furthermore, the synthesis of MgO from these two sources has not been able to generate the quantities needed worldwide (Sabouri et al., 2022). Therefore, researchers are finding alternate ways of increasing the production of Mg and its compound stocks from alternative raw materials to meet their ever-increasing demand (Jassim et al., 2020). The price of MgO has been souring on the global market due to demand surpassing supply of the MgO commodity (Nobre et al., 2020). Therefore, there is a high research drive in the production of MgO in order to make the product affordable and hence for its continuous use in low-end applications. Fernández (2022) has projected an annual production increase of 1.5% between the period of 2020 to 2029. A lot of research is currently ongoing to close the demand-supply gap and hence the increasing world prices.

Recently, a plant-mediated pathway for synthesizing metal oxide has received much attention due to their environmental benign when compared to conventional methods (Mesías et al., 2013; Mousavi et al., 2019; Yusufoğlu et al., 2020). Several plant-based sources of magnesium have been utilized for the synthesis of MgO. For instance, Tabrez et al. (2022) investigated the anticancer efficacy of biogenic synthesized MgONPs by using Cucurbita maxima pumpkin seeds by utilizing a filtered pumpkin seed extract obtained from reflux of powdered seeds in deionized water as their reducing agent. However, there are issues when it comes to their yield and the quality of the MgO produced. Therefore, there is a need to study alternative sources of magnesium for the synthesis of MgO. To the best of our knowledge, there is no study on the synthesis of MgO from *Cucurbita pepo* (pumpkin) seeds for a precursor solution as a reducing agent.

*Cucurbita* species (Pumpkins) are among the top 10 widely grown vegetables in the world (Rolnik & Olas, 2020). Among their wide varieties, *Cucurbita pepo* (Linn) has the most monetary value and is also the commonest *Cucurbita* species grown in Ghana (Abbiw, 1990; Glew et al., 2006). The flesh of pumpkins has been used for decades for food and medicinal purposes (Glew et al., 2006). Their seeds, however, have been viewed as waste and are dumped in landfills or as animal feed. With the advent of nutritional composition studies, *C. pepo* seeds have been discovered to be rich in nutrients, particularly magnesium (Badu et al., 2020; Kwiri, 2014). Since then, there has been a rise in the consumption of these seeds in food and medicine (Devi et al., 2018; Glew et al., 2006). Consumption, however, in Ghana and several other African countries is still significantly low, with the seeds still mainly treated as waste (Badu et al., 2020). In meeting the UN Sustainable Development Goals (SDG12 Responsible consumption and production), instead of discarding as waste, the Mg-rich *C. pepo* seeds can serve as a unique source of MgO for various practical applications. This study, therefore, seeks to investigate the extraction and synthesis of MgO from *Cucurbita pepo* (pumpkin) seeds.

## 2. Methods

De-hulled *C. pepo* seeds were obtained from a seed shop in Techiman, a town in the Bono-East Region of Ghana. Sodium hydroxide (NaOH) pellets and hydrochloric acid (HCl) (70%w/v) used in this study were purchased from VWR Chemicals (France). De-ionized water was used throughout the experiment.

### 2.1. Preparation of magnesium precursor

Seed preparation was done using the approach adopted by Bitog et al. (2009). The fresh seeds were first weighed on a Sartonous BP 6100 model electronic mass balance as initial weight ($W_1$). They were then cleaned and dried in an oven at 105°C for 24 h. The final weight ($W_2$) was recorded. The seeds were then ground in a porcelain mortar and pestle. A portion of the ground seed samples was taken for physicochemical analysis, and the rest were ashed in a Nabertherm muffle furnace at 550°C for 6 h. The resultant ash was weighed and stored in airtight bags for further processing and analysis.

The process by which the magnesium precursor was prepared was adapted from Royani et al. (2018). The

pumpkin seed ash samples were washed with de-ionized water in a hot water bath at 60°C for 2 h. The solution was then filtered with a Whatman No. 1 filter paper, and the residue (seed ash) was dried at 105°C for 3 h. Thereafter, the dried seed ash was added to 2.0 M HCl at a liquid-to-solid ratio of 20 ml/g, with constant stirring at 400 rpm at 75°C for 3 h. The mixture was then filtered with a Whatman No.1 paper afterwards, and the filtrate, which is the magnesium precursor was stored for the magnesium oxide (MgO) synthesis.

### 2.2. Synthesis of magnesium oxide

A 2.0 M NaOH solution was prepared by dissolving NaOH pellets in distilled water. A total of 1.0 L of the solution was prepared. The process of synthesis was adapted from Daisy et al. (2015). The prepared Mg precursor solution (i.e. the leached ash from the *C. pepo* seeds) was added to the NaOH solution in a volume ratio of 1:1. After the formation of a white precipitate ($Mg(OH)_2$), the solution was heated at 100°C for 1 h. Afterwards, the solution was cooled and the $Mg(OH)_2$ was observed to settle at the bottom. The solution was filtered with a Whatman No. 1 filter paper and the precipitate was washed with de-ionized water several times until all water-soluble compounds had been removed. The washed $Mg(OH)_2$ precipitate was then dried and calcined in a muffle furnace at 550°C for 4 h to obtain the MgO. The MgO was transferred into a tight-lid vial and stored in a desiccator for further analysis. The yield of the synthesized MgO was calculated as:

$$MgOyield(\%) = \frac{\text{Mass of product(MgO)obtained}}{\text{Mass of Ash obtained}} \times 100\%$$

### 2.3. Characterization of C. pepo seeds

Proximate composition (moisture and ash content, volatile matter, fixed carbon) was conducted according to García et al. (2013). The macro elements (phosphorus, magnesium, calcium, sodium, and potassium) of the *Cucurbita pepo* seeds were determined according to the method proposed by Rafiu (2012). Nitrogen (N) content was determined by the Kjeldahl method (Rafiu, 2012). Sulfur (S) content was determined by the turbidimetric method (Motsara & Roy, 2008). Walkley–Black wet oxidation method was used to determine Organic carbon (C) (Nelson & Sommers, 1983). The exchangeable acidity titrimetric method according to Mclean (1965) was used to determine the hydrogen (H) content. Oxygen was calculated as %Oxygen = 100 − %(C + H + N). Heavy metals (Pb, Fe, As, Cd, Cr, Hg, Cu, and Ni) in the *C. pepo* seeds were analyzed by an atomic absorption spectrophotometer (AAS), using a tri-acid mixture ($HClO_4$ – $HNO_3$ – HCl) in a volume ratio of 1:2:3 (Kimbrough & Wakakuwa, 1989).

### 2.4. Characterization of the As-synthesized MgO

X-ray fluorescence (XRF) analysis was conducted on the powdered MgO sample using a Philips PW2400 X-ray sequential spectrophotometer to determine their elemental constituents. X-ray diffraction (XRD) analysis on the MgO was conducted using a PAN analytical Empyrean Series machine. The analysis was carried out with CuKα radiations at 45 kV and 40 mA 2θ range scanned from 5° to 99°, step 0.1050, and a counting time of 47 s. The mineral phase was identified using the X'Pert Highscore software package. Fourier-transform infrared (FTIR) analysis was performed in the range of 4000–400 $cm^{-1}$ to detect and analyze the functional groups present in the MgO particles by an FTIR Spectrometer (Amina et al., 2020). The average crystallite size of MgO was determined using the Debye–Scherrer formula (Dobrucka, 2016).

$$D = \frac{K\lambda}{\beta cos\theta} \quad \text{Eq.2}$$

where $D$ is the nanoparticle crystalline size, $K$ denotes the Scherrer constant (0.98), λ represents the wavelength, and β is the full width at half maximum.

### 2.5. Analytical instruments

Physicochemical parameters (pH, EC, temperature, sulfate) were measured by their respective glass electrodes into filtrates of a MgO/water solution in a ratio of 1:10 (w/v) (PC 300 series—Cyber scan) (Islam et al., 2017; Sey & Belford, 2019). $SO_4^{2-}$ determination was adapted from Besseah (2011). This was done by inserting a HACH DR 4000 spectrophotometer (wavelength = 450 nm) into supernatants of 1:5 MgO/water suspensions mixed with Sulfa Ver. 4 reagent powder. All readings were taken on three counts/times.

Citric acid test (CAT) was conducted according to Strydom et al. (2005) to determine the reactivity of the produced MgO. The test measures the time it will take for MgO to neutralize an acid, by causing a change in the pH of a solution to 9 (de Valle-Zermeño et al., 2015). The test was done by adding phenolphthalein drop by drop into a 1:50 solution of MgO and 0.40 N citric acid solution. A color change from white to pink (at pH = 9) indicates the completion of the reaction (Strydom et al., 2005). ANC test was conducted according to DEL Valle-Zermeño et al. (2015).

Acid neutralization capacity (ANC) evaluates the ability of the synthesized MgO particles to provide a buffer pH range which ensures minimum solubility of acids over a period (DEL Valle-Zermeño et al., 2015). This was done by determining the volume of acid (1.0 M $HNO_3$, 65 wt%) that was needed to drop the pH of the MgO solution from that of minimum solubility (pH ≥ 9) to pH that allows metal redissolution (pH ≤ 4).

Heavy metal concentrations of the produced MgO were determined according to EPA Method 3050 B (SW-846). The analysis was done by digesting 1 g of MgO with a tri-acid mixture ($HClO_4$, $HNO_3$, and HCl) in a 1:2:3 ratio. The concentrations of (Fe, Pb, Cu, Cd, Ni, Cr, Hg, and As) were analyzed by an atomic absorption spectrophotometer (SPECTRA AA 220 Air-acetylene Flame)

## 3. Results and discussion

### 3.1. Proximate and elemental composition of C. pepo seeds

The average moisture content (%MC) recorded for the *C. pepo* seeds was 5.63 ± 0.06% as shown in Table 1. Similar values were recorded by Kwiri (2014) and STEINER-ASIEDU et al. (2014), with a slightly higher value recorded by Badu et al. (2020). Bowman and Barringer (2012) reported that the %MC of *C. pepo* seeds can be as high as 50%. Given the comparatively lower %MC in this study, it can be implied that the *C. pepo* seeds were dry. Generally, ash content of biomass is reported in published studies to be low (Zając et al., 2018), and in this study, *C. pepo* seeds produced low quantities of ash (4.31 ± 0.29%). The obtained value was similar to STEINER-ASIEDU et al. (2014) and Badu et al. (2020), but higher than Kwiri (2014).

The average volatile matter (%VM) of the seeds was recorded as 93.46 ± 0.99%. *C. pepo* seeds have notably high volatile matter content (>70%) as recorded by literature, due to high levels of fatty acids and oil (Bowman & Barringer, 2012; Zając et al., 2018). Bowman and Barringer (2012) also reported that a low %MC in the seeds resulted in higher %VM and vice versa, which was confirmed in this study. The average fixed carbon content (%FC), which determines the biochar left after combustion, was recorded at 2.22 ± 1.28% in conformance with Zając et al. (2018). %FC is also dependent on the %VM, as a high %VM is indicative of a low %FC, as observed in this study.

The elemental composition of the ashed-seed is presented in Table 2. Average Carbon (C) content was high as 50.21 ± 0.90%. This is similar to Bitog et al. (2009) who noted that biomass has high C content. Relatively lower values of Hydrogen (H) and Nitrogen (N) were recorded in this study. This is because H content vaporizes in combustion and the N content does not combust in temperatures less than 1000°C (Bitog et al., 2009). Sulfur (S) content was expectedly low and was recorded as 0.07 ± 0.01%.

*C. pepo* seeds are notably rich in various minerals. Constituent major minerals for this study are presented in Table 3. Mineral concentration was in the increasing order of sodium < magnesium < calcium < potassium < phosphorus. The results obtained were consistent with Sinkovič et al. (2021) who also recorded higher concentrations of phosphorus (1125 mg/100 g) and potassium (860 mg/100 g). Several other works also recorded higher concentrations of P and K (Glew et al., 2006; Kwiri, 2014; Rezig et al., 2019; Seymen et al., 2016).

Magnesium content (250 mg/100 g) recorded in this study was within the range reported by Seymen et al. (2016) (127.52–393.82 mg/100 g). The recorded value was higher than that of Elinge et al. (2012) (67.41 mg/100 g) and Hashash et al. (2017) (60.4 mg/100 g). Mg content was, however, slightly lower than Kwiri (2014) (344.6 mg/100 g), STEINER-ASIEDU et al. (2014) (530 mg/100 g), Rezig et al. (2019) (527.8 mg/100 g), and Badu et al. (2020) (313.63 mg/100 g). Kwiri (2014) noted that the mineral concentration of seeds is dependent on location and climate conditions, hence the variation.

**Table 2.** Average elemental composition of *C. pepo* seeds

| Element | Average Composition (%) |
|---|---|
| Carbon (C) | 5.21 ± .90 |
| Hydrogen (H) | 8.18 ± .17 |
| Nitrogen (N) | 4.59 ± .11 |
| Sulfur (S) | .07 ± .01 |

Values are expressed as Mean ± standard error of the mean

**Table 1.** Average proximate composition of *C. pepo* seeds

| Parameters | Average Composition (%) | Other Studies | References |
|---|---|---|---|
| Moisture Content | 5.00 ± .00 | 5.2, 5.662 | (Gohari et al., 2013; Kwiri, 2014) |
| Ash Content | 4.31 ± .29 | 2.49, 3.324 | (Gohari et al., 2013; Kwiri, 2014) |
| Volatile Matter | 83.48 ± .99 | 70 | (Hagos et al., 2022) |
| Fixed Carbon | 7.21 ± 1.28 | 17.5 | (Demiral & Şamdan, 2016) |

Values are expressed as Mean ± standard error of the mean

**Table 3.** Major minerals in *C. pepo* seeds

| | Average Composition | |
|---|---|---|
| Element | (%) | (mg/100 g) |
| Phosphorus (P) | 1.29 ± 0.00 | 1290 ± 0.00 |
| Potassium (K) | 0.92 ± 0.00 | 920 ± 0.00 |
| Sodium (Na) | 0.04 ± 0.00 | 40 ± 0.00 |
| Calcium (Ca) | 0.66 ± 0.07 | 660 ± 0.07 |
| Magnesium (Mg) | 0.25 ± 0.03 | 250 ± 0.03 |

Values are expressed as Mean ± standard error of the mean

## 3.2. Characterization of synthesized MgO

### 3.2.1. Physicochemical composition

The percentage yield (%) of MgO was calculated as 23%. In this study, the pH of MgO recorded in Table 4 was relatively high (10.63 ± 0.21) which is consistent with values obtained by (DEL Valle-Zermeño et al., 2015; GARCIA et al., 2004; Shen et al., 2019). This value confirms MgO as a strong basic oxide that can be effective for purposes like soil remediation due to its high alkalinity. EC of the MgO was relatively high (2930 ± 26.46 µS/cm), signifying the presence of many mobile inorganic ions.

Miller and Curtin (2006) noted that the conductivity of a solution is dependent on the concentration of all the constituent ions and the types of those ions. They noted that higher ion concentrations, particularly inorganic, resulted in a higher conductivity value. Inorganic ions such as $Na^+$, $K^+$, $Mg^{2+}$, $Ca^{2+}$, $HCO^{3-}$, $Cl^-$, and $SO_4^{2-}$ are strong electrolytes, due to the ease of complete dissociation. Thus, the synthesized MgO particles may contain a high concentration of these ions, thus its high EC value. The temperature of MgO was recorded at 27.77 ± 0.86°C. Temperature is relevant for the movement of ions in a medium and facilitates chemical reactions (Onwuka & Mang, 2018). This is an essential property for works concerning stabilization and photocatalysis. Sulphate concentration (mg/L) was recorded as low as 0.014 ± 0.00.

**Table 4.** Physicochemical properties of synthesized MgO

| Properties | Measured Value |
|---|---|
| pH | 10.63 ± 0.21 |
| E.C (µs/cm) | 2930 ± 26.46 |
| Temperature (°C) | 27.78 ± 0.86 |
| Sulphate (SO4 2-) (mg/L) | 0.014 ± 0.00 |

### 3.2.2. Presence of functional groups in the synthesized MgO

In this study, the FTIR profile of MgO displayed five main bands assigned to different functional groups (Figure 1(a)). The broad band at 3461 $cm^{-1}$ represents the stretching frequency of the O–H bond (3500–3200 $cm^{-1}$), which is due to the formation of an alcoholic compound along with MgO in synthesis (Jeevanandam et al., 2017). This bond may also represent residual water molecules from the reducing agent solution for synthesis (Ashok et al., 2016; Kandiban et al., 2015). The band around 1600 $cm^{-1}$ according to Ashok et al. (2016) represents an endothermic peak due to the weak stretching vibration of water molecules. In this study, however, this peak could represent the N-H bend (primary amine), due to the presence of the amino acid Lysine, which is present in *C. pepo* seeds (Devi et al., 2018; Jeevanandam et al., 2017).

The band around 1400 $cm^{-1}$ is representative of O–H bending vibration according to (Amina et al., 2020). C=O stretching frequency is observed at the broadband at 1381 $cm^{-1}$ which denotes the presence of an aromatic ring (Kandiban et al., 2015). The peak at 584 $cm^{-1}$ in the range of 660–540 $cm^{-1}$ represents Mg-O stretching, which signifies the formation of MgO (Amina et al., 2020; Ashok et al., 2016; Jeevanandam et al., 2017; Kandiban et al., 2015).

The major mineralogical phases in the MgO powder were identified by XRD analysis in Figure 1(b). In Figure 1(b), the major phases present are MgO and NaCl. This result confirms the high EC value obtained

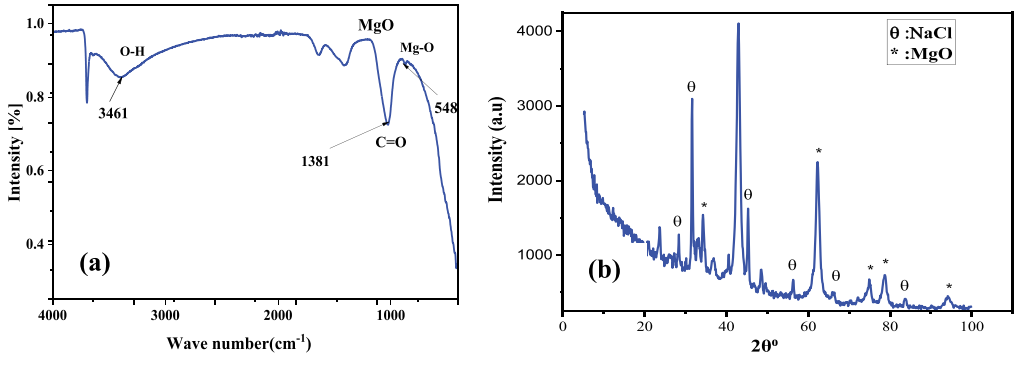


**Figure 1.** (A) FTIR Spectrum and (b) X-ray diffraction (XRD) pattern of synthesized MgO from *C. pepo* seeds.

for the particles (Section 3.2.2) which implied a high concentration of mobile ions such as $Mg^{2+}$, $Na^{+}$, $O^{2-}$, and $Cl^{-}$.

The synthesized MgO particles are of a cubic structure and crystalline nature. MgO was present in its crystalline form Periclase, with diffraction peaks at 36.78°, 42.88°, 62.24°, 74.98°, 78.83°, and 93.10°. These peaks are representative of the (111), (200), (220), (311), (222), and (400) crystal planes, respectively. These planes are characteristic of MgO as recorded by several studies (Amina et al., 2020; Camtakan et al., 2012; Jhansi et al., 2017; Mantilaka et al., 2014). Identified peaks were almost similar to that obtained by Jhansi et al. (2017) and Balakrishnan et al. (2020). From Figure 1(b), it is observed that the highest intensity peak is obtained at 42.88°, representing the (200) planes of MgO, consistent with MgO diffraction analysis in literature.

The average crystallite size was determined from the most intense peak (42.88°) using the Debye–Scherrer equation as 26 nm. Camtakan et al. (2012) recorded a close value of 24 nm when they synthesized MgO using $MgCl_2$ and NaOH. The value was also nearly similar to that of Krishnamoorthy et al. (2012) (25–27 nm) who synthesized MgO using neem leaves. Amina et al. (2020) recorded higher crystallite sizes of 30 nm and 34 nm in their study using Indian Wood Costus and Sea Incense Costus. Lesser sizes were, however, recorded by Jhansi et al. (2017) (15–20 nm) and Dobrucka (2016) (10 nm).

Generally, crystallite size is inversely proportional to peak width-FWHM (β) (Speakman, 2014). This was confirmed by increasing crystallite size with decreasing β values obtained from the XRD spectrum data, as well as the narrow peaks observed in Figure 1(b). Crystallite size also increases by increasing calcination temperature (Krishnamoorthy et al., 2012; Pilarska et al., 2017; Tang & LV, 2014). The authors noted that calcination temperature above 800°C increased crystallite size. Calcination temperature employed in this study was lower (500°C), hence the smaller crystallite size.

Sodium Chloride (NaCl) was present as Halite and was identified in the synthesized particles as impurities. The constituent NaCl may have been produced from the reaction between the NaOH used as the reducing agent and the HCl used as the leaching medium of the seed ash. NaCl content can be reduced by extended washing of $Mg(OH)_2$ precipitate before calcination.

### 3.2.3. Reactivity of the synthesized MgO

In this study, the time for color change at pH 9 was recorded as 2 seconds (s). The obtained reactivity (s) value was categorized as highly reactive according to Strydom et al. (2005). The reactivity time obtained implies that the produced MgO can raise the pH of a system to 9, where acid is neutralized at a fast rate. In practice, this quality is highly desirable in areas such as heavy metal stabilization, where there is a need for a shorter remediation time. The value recorded was significantly lower than DEL Valle-Zermeño et al. (2015) who recorded >810 s for LG-MgO, Shen et al. (2019) at 33–3322 s, and GIRO-Paloma et al. (2020) at 60–1320 s. Reactivity also informs about the specific surface area of the MgO, and the higher the reactivity, the greater the surface area. Reactivity is also dependent on calcination temperatures for MgO. The higher the calcination temperature, the lower the surface area and the lower the reactivity (GIRO-Paloma et al., 2020; Shen et al., 2019). In this study, calcination was done at a low temperature of 500°C, hence the high reactivity of the MgO.

### 3.2.4. Acid neutralization capacity of the synthesized MgO

The results of the ANC of the MgO, which is presented as a curve of pH against hydronium ($H_3O^{+}$) per mass of solid are shown in Figure 2. From Figure 2, three phases of the ANC curve and equilibrium were established. The first phase was observed in a pH range between 11.1 and 10.05 and the second phase was marked by a pH between 10.05 and 8 over a wide range of acid additions. The last phase was observed from pH 8 to 4. It is noteworthy that some alkali species present in the MgO establish a solubility equilibrium when they come into contact with water, and form their corresponding hydroxides. The composition of oxide is crucial to and affects the ANC curve results. This is because the hydroxides of metals are that which are involved in solubility control reactions (GIRO-Paloma et al., 2020).

The pH of the synthesized powder started from 11.1, which is higher than the natural pH of MgO (<11). This is due to the presence of CaO in the particles as shown in Table 2, whose hydroxide ($Ca(OH)_2$) controlled the solubility of the first phase. A drop in pH caused by an addition of a small amount of nitric acid (mol $H_3O^{+}$) brought the pH to 10.05, at which stage solubility is controlled by the hydration product of MgO ($Mg(OH)_2$/brucite). The takeover of solubility from $Ca(OH)_2$ by $Mg(OH)_2$ was fast due to the high reactivity of the produced MgO. There is also the possibility that added acid ($HNO_3$) quickly consumed the CaO in the first stage (GIRO-Paloma et al., 2020).

From pH of 10.05, the second phase was exclusively controlled by the solubility equilibrium of $Mg(OH)_2$, which acted as a buffering agent over a long range of acid ($HNO_3$) additions as shown in Figure 2. DEL Valle-

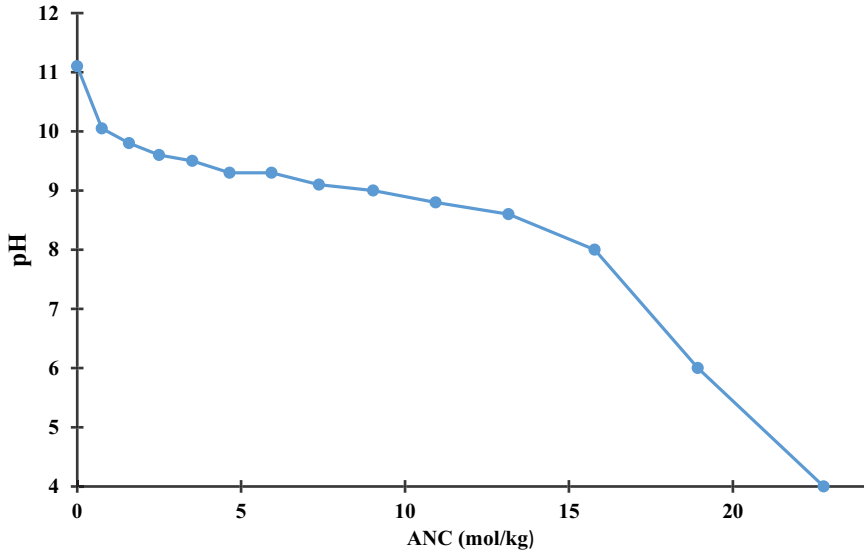


**Figure 2.** Acid neutralization capacity (ANC) of produced MgO.

Zermeño et al. (2015) noted that hydration reactions easily reach equilibrium and slow down neutralizing reaction rates. It can be observed that acid consumption of the MgO was considerably high, especially in the range between the natural pH (10.5) and pH 8, at which point a gradual drop was observed, with a similar observation noted by DEL Valle-Zermeño et al. (2015) and GIRO-Paloma et al. (2020).

The third phase of the ANC results was marked by a descending curve in the pH 8–4 range. As pH fell below 8, solubility became more prominent and may have resulted from the dissolution of some metal hydroxides such as $Zn(OH)_2$. Low pH at this phase may have also been controlled by the solubility of $H_3PO_4$ which was present in the oxide powder. It is worth noting that the $Al_2O_3$, $SiO_2$, and $Fe_2O_3$ present in the MgO particles did not influence the ANC curve since they remain inert in their precipitated forms (GARCIA et al., 2004; GIRO-Paloma et al., 2020).

It can be inferred from the foregoing, that MgO provides a buffer at a pH range of 8–10.05, where it can resist pH changes for consecutive acid additions till pH drops. ANC required to exceed minimum solubility (pH 8.5–10.5) was 15.78 $mol^+/kg$. To further lower the pH to 4, where redissolution of acids may occur, ANC required was high at 22.77 $mol^+/kg$. GIRO-Paloma et al. (2020) recorded ANC values of 16–25 $mol^+/kg$ in their comparative studies of low-grade MgO. Upper limits of ANC values are set at ≥20 $mol^+/kg$ (Ayensu et al., 2020; Wahlström et al., 2009). In this regard, the produced MgO had a high neutralizing capacity and can provide a stable pH range of minimum solubility over a long time against acidification.

### 3.2.5. Heavy metal concentrations in the synthesized MgO

The concentration of selected heavy metals analyzed in this study is presented in Table 5. The values obtained were very low, compared to standard limits set by WHO (1996). It can thus be implied that the concentrations are not high enough to confer significant degrees of toxicity when utilized for further purposes such as soil stabilization and toxic metal adsorption. The synthesized powder can thus be employed in areas such as contaminated soil and wastewater remediation.

### 3.2.6. Chemical composition of the synthesized MgO particles

The chemical composition of the synthesized MgO is presented in Table 6. From the table, the produced MgO powder contained magnesium oxide (MgO) as the most dominant oxide at 75.1%. This confirms the formation and successful synthesis of MgO from *C. pepo* seeds.

**Table 5.** Concentrations of heavy metals in the synthesized MgO

| Metal | Average Concentration (mg/kg) | WHO (1996) Limit (mg/kg) |
|---|---|---|
| Fe | 34.47 ± 1.10 | 350 |
| Cu | 12.9 ± 0.53 | 36 |
| Cd | 0.04 ± 0.00 | 0.8 |
| Ni | 0.01 ± 0.00 | 35 |
| Pb | 0.02 ± 0.00 | 85 |
| Hg | 0.01 ± 0.00 | 0.03 |
| As | 0.03 ± 0.00 | 40 |
| Cr | 0.01 ± 0.00 | 100 |

Values are expressed as Mean ± standard error of the mean

**Table 6.** Chemical composition of synthesized MgO

| Element | MgO | $P_2O_5$ | CaO | $Fe_2O_3$ | $SiO_2$ | ZnO | $Al_2O_3$ | MnO | $ZrO_2$ | CuO |
|---|---|---|---|---|---|---|---|---|---|---|
| Conc. (%) | 75.1 | 9.58 | 8.26 | 1.64 | 1.55 | 1.29 | 1.24 | 0.68 | 0.34 | 0.14 |

This percentage of MgO (75.1%) is significantly higher than the values for low-grade MgO (42.9%) obtained from the calcination of natural magnesite used by GARCIA et al. (2004).

Phosphorus oxide ($P_2O_5$) and calcium oxide (CaO) were present in relatively lower concentrations at 9.58% and 8.26%, respectively. Other constituents were also present, albeit in very low concentrations; iron oxide ($Fe_2O_3$), silica ($SiO_2$), zinc oxide (ZnO), aluminum oxide ($Al_2O_3$), manganese oxide (MnO), zirconium dioxide ($ZrO_2$) and copper oxide (CuO). Low concentrations of sulfite ($SO_3$) confirm the low concentrations of sulfate ($SO_4^{2-}$) recorded in Section 3.2.2 (Seshadri et al., 2016).

There were observable differences in the concentrations of the elements and oxides such as $Fe_2O_3$ and CuO analyzed by AAS and XRF. This may be due to the inert and precipitated states some oxides assume in alkaline conditions (GARCIA et al., 2004; Wahlström et al., 2009), in which regard their concentrations are not observably high.

## 4. Conclusion

This study investigated the production of magnesium oxide (MgO) from *Cucurbita pepo* seeds, as a way of obtaining value from bio-waste, and presenting an economical and environmentally safe MgO for environmental remediation applications. The sample seeds and synthesized MgO were deeply characterized by physicochemical and microscopic analytical methods. The obtained results revealed that the seeds had low quantities of moisture and ash but were high in volatile matter content. The seeds also contained significant quantities of mineral elements, with an Mg concentration of 250 mg/100 g. FTIR analysis confirmed the formation of MgO by the characteristic peak formation in the range of 660–540 $cm^{-1}$. XRF analysis revealed the MgO powder contained 75.1% of MgO out of the total weight. The particles were crystalline with a cubic structure and an average size of 26 nm. The synthesized MgO had a high pH, thus high alkalinity. It was also highly reactive with a reaction time of 2 s and had an ANC value of 22.77 $mol^{+}$/kg, hence a high buffering capacity. Heavy metal analyses also showed that all the metal concentrations in the produced MgO were significantly lower than the WHO limits. Thus, the synthesis of MgO from *C. pepo* seeds was successful and can be used for further waste remediation studies.

## Acknowledgements

The authors wish to express their profound gratitude to Owere Mines Limited for facilitating the assessment of the study site.

## Disclosure statement

The authors declare that they have no known competing financial interests or personal relationships that could have appeared to influence the work reported in this paper.

## Funding

The authors received no funding for the conduct of the study.

## ORCID

Emmanuel Gikunoo http://orcid.org/0000-0003-4382-9997

## Author contribution statement

Patience Oduroa Agyapong was involved in data collection, experimental work, and original draft preparation. Frank Ofori Agyemang and Douglas Siaw Baah were involved in the research design, data analysis, and manuscript review. Daniel Adjah Annan was involved in validation, data analysis, and write-up coordination. Emmanuel Kwesi Arthur, Gordon Foli, and Emmanuel Gikunoo conceptualized the research, were involved in the research design and review of the manuscript and provided the needed supervisory roles.

## Data availability statement

The authors confirm that the data supporting the findings of this study are available within the manuscript.

## References

Abbiw, D. K. (1990). *Useful plants of Ghana*. Intermediate Technology. https://doi.org/10.3362/9781780443737.000

Ahmed, M., & ABOU-GAMRA, Z. (2016). Mesoporous MgO nanoparticles as a potential sorbent for removal of fast orange and bromophenol blue dyes. *Nanotechnology for Environmental Engineering*, *1*(1), 1–11. https://doi.org/10.1007/s41204-016-0010-7

Amina, M., AL Musayeib, N. M., Alarfaj, N. A., EL-Tohamy, M. F., Oraby, H. F., AL Hamoud, G. A., Bukhari, S. I., Moubayed, N. M. S., & Mishra, Y. K. (2020). Biogenic green synthesis of MgO nanoparticles using saussurea costus biomasses for a comprehensive detection of their antimicrobial, cytotoxicity against MCF-7 breast cancer cells

and photocatalysis potentials. *PLoS ONE*, *15*(8), e0237567. https://doi.org/10.1371/journal.pone.0237567

Ashok, C., Rao, K., Chakra, C., & Rao, K. (2016). Mgo nanoparticles prepared by microwave-irradiation technique and its seed germination application. *Nano Trends-A Journal of Nano Technology & Its Applications*, *18*(1), 10–17.

Ayensu, I., Bekoe, S. O., Adu, J. K., Brobbey, A. A., & Appiah, E. (2020). Evaluation of acid neutralizing and buffering capacities of selected antacids in Ghana. *Scientific African*, *8*, e00347. https://doi.org/10.1016/j.sciaf.2020.e00347

Badu, M., Pedavoah, M.-M., & Dzaye, I. Y. (2020). Proximate composition, antioxidant properties, mineral content and anti-nutritional composition of Sesamum Indicum, Cucumeropsis Edulis and Cucurbita pepo seeds grown in the savanna regions of Ghana. *Journal of Herbs, Spices & Medicinal Plants*, *26*(4), 329–339. https://doi.org/10.1080/10496475.2020.1747581

Balakrishnan, G., Velavan, R., Batoo, K. M., & Raslan, E. H. (2020). Microstructure, optical and photocatalytic properties of MgO nanoparticles. *Results in Physics*, *16*, 103013. https://doi.org/10.1016/j.rinp.2020.103013

Besseah, M. 2011. *Effects of small scale gold mining on water resources: A case study of Bogoso/Prestea mining area*. PhD ThesisSubmitted to the Board of Postgraduate Studies, Kwame Nkrumah . . . .

Bitog, J. P. P., Elauria, J. C., Elepaño, A. R., & Resurreccion, A. N. (2009). Design fabrication and evaluation of a direct-fired corn cob furnace for corn drying. *Philippines Journal of Agricultural and Biosystems Engineering (Philippines)*, *7*, 3–15.

Bowman, T., & Barringer, S. (2012). Analysis of factors affecting volatile compound formation in roasted pumpkin seeds with selected ion flow tube-mass spectrometry (SIFT-MS) and sensory analysis. *Journal of Food Science*, *77*(1), C51–60. https://doi.org/10.1111/j.1750-3841.2011.02465.x

Camtakan, Z., Erenturk, S., & Yusan, S. (2012). Magnesium oxide nanoparticles: Preparation, characterization, and uranium sorption properties. *Environmental Progress & Sustainable Energy*, *31*(4), 536–543. https://doi.org/10.1002/ep.10575

Daigle, B., & DeCarlo, S. (2022). *Magnesium price spike: A flash in the pan?*. Office of Industries, US International Trade Commission.

Daisy, S. L., Mary, A. C. C., Devi, K., & Santhana, S. (2015). Magnesium oxide nanoparticles-synthesis and charecterisation. *International Journal of Nano Science, Nano Engineering*, *2*(5), 64–69.

DE Baaij, J. H., Hoenderop, J. G., & Bindels, R. J. (2015). Magnesium in man: Implications for health and disease. *Physiological Reviews*, *95*(1), 1–46. https://doi.org/10.1152/physrev.00012.2014

Dehghan, Z., Ranjbar, M., Govahi, M., & Khakdan, F. (2022). Green synthesis of Ag/Fe3O4 nanocomposite utilizing eryngium planum L. leaf extract and its potential applications in medicine. *Journal of Drug Delivery Science and Technology*, *67*, 102941. https://doi.org/10.1016/j.jddst.2021.102941

DEL Valle-Zermeño, R., Giro-Paloma, J., Formosa, J., & Chimenos, J. M. (2015). Low-grade magnesium oxide by-products for environmental solutions: Characterization and geochemical performance. *Journal of Geochemical Exploration*, *152*, 134–144. https://doi.org/10.1016/j.gexplo.2015.02.007

Del Valle-Zermeño R, Niubó, M., Formosa, J., Guembe, M., Aparicio, J. A., & Chimenos, J. M. (2015). Synergistic effect of the parameters affecting wet flue gas desulfurization using magnesium oxides by-products. *Chemical Engineering Journal*, *262*, 268–277.

Demiral, İ., & Şamdan, C. A. (2016). Preparation and characterisation of activated carbon from pumpkin seed shell using H3PO4. *Anadolu University Journal of Science and Technology A-Applied Sciences and Engineering*, *17*(1), 125–138. https://doi.org/10.18038/btda.64281

Devi, N. M., Prasad, R. V., & Sagarika, N. (2018). A review on health benefits and nutritional composition of pumpkin seeds. *International Journal of Chemical Studies*, *6*, 1154–1157.

Dobrucka, R. (2016). Synthesis of MgO nanoparticles using Artemisia abrotanum herba extract and their antioxidant and photocatalytic properties. *Iranian Journal of Science & Technology, Transactions A: Science*, *42*(2), 547–555. https://doi.org/10.1007/s40995-016-0076-x

Elinge, C. M., Muhammad, A., Atiku, F. A., Itodo, A. U., Peni, I. J., Sanni, O. M., & Mbongo, A. N. (2012). Proximate, mineral and anti-nutrient composition of pumpkin (*Cucurbita pepo L)* seeds extract. *International Journal of Plant Research*, *2*, 146–150. https://doi.org/10.5923/j.plant.20120205.02

Fernandes, M., RB Singh, K., Sarkar, T., Singh, P., & Pratap Singh, R. (2020). Recent applications of magnesium oxide (MgO) nanoparticles in various domains. *Advanced Materials Letters*, *11*(8), 1–10. https://doi.org/10.5185/amlett.2020.081543

Fernández, L. (2022). Global magnesium oxide market volume 2015-2029. *Statista*. https://www.statista.com/statistics/1310514/magnesium-oxide-market-volume-worldwide/

Fouda, A., Hassan, S. E.-D., Saied, E., & Hamza, M. F. (2021). Photocatalytic degradation of real textile and tannery effluent using biosynthesized magnesium oxide nanoparticles (MgO-NPs), heavy metal adsorption, phytotoxicity, and antimicrobial activity. *Journal of Environmental Chemical Engineering*, *9*(4), 105346. https://doi.org/10.1016/j.jece.2021.105346

Garcia, M. A., Chimenos, J. M., Fernandez, A. I., Miralles, L., Segarra, M., & Espiell, F. (2004). Review of scientific literature on the use of stabilisation/solidification for the treatment of contaminated soil, solid waste and sludges. *Chemosphere*, *56*(5), 481–491. https://doi.org/10.1016/j.chemosphere.2004.04.005

García, R., Pizarro, C., Lavín, A. G., & Bueno, J. L. (2013). Biomass proximate analysis using thermogravimetry. *Bioresource Technology*, *139*, 1–4. https://doi.org/10.1016/j.biortech.2013.03.197

GIRO-Paloma, J., Formosa, J., & Chimenos, J. M. (2020). Stabilization study of a contaminated soil with metal(loid)s adding different low-grade MgO degrees. *Sustainability*, *12*(18), 12. https://doi.org/10.3390/su12187340

Glew, R., Glew, R., Chuang, L.-T., Huang, Y.-S., Millson, M., Constans, D., & Vanderjagt, D. (2006). Amino acid,

mineral and fatty acid content of pumpkin seeds (Cucurbita spp) and Cyperus esculentus nuts in the Republic of Niger. *Plant Foods for Human Nutrition*, *61* (2), 49–54. https://doi.org/10.1007/s11130-006-0010-z

Gohari, A. A., Farhoosh, R., & Haddad, K. M. (2013). Chemical composition and physicochemical properties of pumpkin seeds (Cucurbita pepo subsp. pepo var. Styriaka) grown in Iran. *Journal Agric Science and Technology*, *13*, 1053–1063.

Guerrera, M. P., Volpe, S. L., & Mao, J. J. (2009). Therapeutic uses of magnesium. *American Family Physician*, *80*(2), 157–162.

Gysau, D. (2006). *Fillers for paints: Fundamentals and applications*. Vincentz Network GmbH & Co KG.

Hagos, M., Yaya, E. E., Chandravanshi, B. S., & Redi-Abshiro, M. (2022). Analysis of volatile compounds in flesh, peel and seed parts of pumpkin (Cucurbita maxima) cultivated in Ethiopia using gas chromatography-mass spectrometry (GC-MS). *International Journal of Food Properties*, *25*(1), 1498–1512. https://doi.org/10.1080/10942912.2022.2088787

Hashash, M. M., EL-SAYED, M. M., ABDEL-HADY, A. A., Hady, H. A., & Morsi, E. A. (2017). Nutritional potential, mineral composition and antioxidant activity squash (Cucurbita pepo l.) fruits grown in EGYPT. *Inflammation*, *9*(10).

Hornak, J. (2021). Synthesis, properties, and selected technical applications of magnesium oxide nanoparticles: A review. *International Journal of Molecular Sciences*, *22*(23), 12752. https://doi.org/10.3390/ijms222312752

HØY-Petersen, N., & Rizley, J. H. 2020. Magnesium processing. *Encyclopedia Britannica*. Britannica.

Islam, M. N., Taki, G., Nguyen, X. P., JO, Y.-T., Kim, J., & Park, J.-H. (2017). Heavy metal stabilization in contaminated soil by treatment with calcined cockle shell. *Environmental Science and Pollution Research*, *24*(8), 7177–7183. https://doi.org/10.1007/s11356-016-8330-5

Jamil, N., Mehmood, M., Lateef, A., Nazir, R., & Ahsan, N. (2015). MgO nanoparticles for the removal of reactive dyes from wastewater. *Advanced Materials-TechConnect Briefs*, *1*, 353–356.

Jassim, A., Salmtori, S., & Jassam, J. (2020). Sustainable manufacturing process applied to produce magnesium oxide from sea water. *Materials Science and Engineering*, *757*(1), 012021. https://doi.org/10.1088/1757-899X/757/1/012021

Jeevanandam, J., Chan, Y. S., & Danquah, M. K. (2017). Biosynthesis and characterization of MgO nanoparticles from plant extracts via induced molecular nucleation. *New Journal of Chemistry*, *41*(7), 2800–2814. https://doi.org/10.1039/C6NJ03176E

Jhansi, K., Jayarambabu, N., Reddy, K. P., Reddy, N. M., Suvarna, R. P., RAO, K. V., Kumar, V. R., & Rajendar, V. (2017). Biosynthesis of MgO nanoparticles using mushroom extract: Effect on peanut (Arachis hypogaea L.) seed germination. *Biotechnology*, *7*(4), 1–11. https://doi.org/10.1007/s13205-017-0894-3

Julkapli, N. M., & Bagheri, S. (2016). Magnesium oxide as a heterogeneous catalyst support. *Reviews in Inorganic Chemistry*, *36*(1), 1–41. https://doi.org/10.1515/revic-2015-0010

Kalita, C., Sarkar, R. D., Verma, V., Bharadwaj, S. K., Kalita, M. C., Boruah, P. K., Das, M. R., & Saikia, P. (2021). Bayesian modeling coherenced green synthesis of NiO nanoparticles using camellia sinensis for efficient antimicrobial activity. *BioNanoscience*, *11*(3), 825–837. https://doi.org/10.1007/s12668-021-00882-x

Kandiban, M., Vigneshwaran, P., & Potheher, I. V. (2015). Synthesis and characterization of mgo nanoparticles for photocatalytic applications. *Proceedings of the National Conference on Advances in Crystal Growwth and Nanotechnology*, India.

Kimbrough, & Wakakuwa. (1989). Acid digestion for sediments, sludges, soils, and solid wastes. A proposed alternative to EPA SW 846 method 3050. *Environmental Science & Technology*, *23*(7), 898–900. https://doi.org/10.1021/es00065a021

Krishnamoorthy, K., Manivannan, G., Kim, S. J., Jeyasubramanian, K., & Premanathan, M. (2012). Antibacterial activity of MgO nanoparticles based on lipid peroxidation by oxygen vacancy. *Journal of Nanoparticle Research*, *14*(9), 1–10. https://doi.org/10.1007/s11051-012-1063-6

Kulekci, M. K. (2008). Magnesium and its alloys applications in automotive industry. *The International Journal of Advanced Manufacturing Technology*, *39*(9–10), 851–865. https://doi.org/10.1007/s00170-007-1279-2

Kwiri, R. (2014). Proximate composition of pumpkin gourd (Cucurbita pepo) seeds from Zimbabwe. *International Journal of Nutrition and Food Sciences*, *3*(4), 279. https://doi.org/10.11648/j.ijnfs.20140304.17

Mantilaka, M., Pitawala, H., Karunaratne, D., & Rajapakse, R. (2014). Nanocrystalline magnesium oxide from dolomite via poly (acrylate) stabilized magnesium hydroxide colloids. *Colloids and Surfaces A: Physicochemical and Engineering Aspects*, *443*, 201–208. https://doi.org/10.1016/j.colsurfa.2013.11.020

Mclean, E. (1965). Aluminum. *Methods of Soil Analysis: Part2 Chemical and Microbiological Properties*, *9*, 978–998. https://doi.org/10.2134/agronmonogr9.2.c16

Mesías, M., Navarro, M., Gökmen, V., & Morales, F. J. (2013). Antiglycative effect of fruit and vegetable seed extracts: Inhibition of AGE formation and carbonyl-trapping abilities. *Journal of the Science of Food and Agriculture*, *93*(8), 2037–2044. https://doi.org/10.1002/jsfa.6012

Miller, J. J. & Curtin, D. (2006). Soil Sampling and Methods of Analysis. In Carter, M. R., & Gregorich, E. G. (Eds.), *Canadian Society of Soil Science* (2nd ed) (p. 12). Taylor & Francis Group, LLC.

Mohamed, A. A., ABU-Elghait, M., Ahmed, N. E., & Salem, S. S. (2021). Eco-friendly mycogenic synthesis of ZnO and CuO nanoparticles for in vitro antibacterial, antibiofilm, and antifungal applications. *Biological Trace Element Research*, *199*(7), 2788–2799. https://doi.org/10.1007/s12011-020-02369-4

Mori, H., Tack, J., & Suzuki, H. (2021). Magnesium oxide in constipation. *Nutrients*, *13*(2), 421. https://doi.org/10.3390/nu13020421

Motsara, M., & Roy, R. N. (2008). *Guide to laboratory establishment for plant nutrient analysis*. Food and Agriculture Organization of the United Nations Rome.

Mousavi, S. M., Hashemi, S. A., Ramakrishna, S., Esmaeili, H., Bahrani, S., KooshA, M., & BabapooR, A. (2019). Green synthesis of supermagnetic Fe3O4–MgO nanoparticles via nutmeg essential oil toward superior anti-bacterial and anti-fungal performance. *Journal of Drug Delivery Science*

*and Technology*, *54*, 101352. https://doi.org/10.1016/j.jddst.2019.101352

Nagappa, B., & Chandrappa, G. (2007). Mesoporous nanocrystalline magnesium oxide for environmental remediation. *Microporous and Mesoporous Materials*, *106* (1–3), 212–218. https://doi.org/10.1016/j.micromeso.2007.02.052

Nelson, D. A., & Sommers, L. E. (1983). Total carbon, organic carbon, and organic matter. *Methods of Soil Analysis: Part 2 Chemical and Microbiological Properties*, *9*, 539–579. https://doi.org/10.2134/agronmonogr9.2.2ed.c29

Nobre, J., Ahmed, H., Bravo, M., Evangelista, L., & DE Brito, J. (2020). Magnesia (MgO) production and characterization, and its influence on the performance of cementitious materials: A review. *Materials*, *13*(21), 4752. https://doi.org/10.3390/ma13214752

Onwuka, B., & Mang, B. (2018). Effects of soil temperature on some soil properties and plant growth. *Advances in Plants & Agriculture Research*, *8*(1), 34–37. https://doi.org/10.15406/apar.2018.08.00288

Pilarska, A. A., Klapiszewski, Ł., & Jesionowski, T. (2017). Recent development in the synthesis, modification and application of Mg(OH)2 and MgO: A review. *Powder Technology*, *319*, 373–407. https://doi.org/10.1016/j.powtec.2017.07.009

Rafiu, S. 2012. *The potential of Azadirachta indica leave biomass as a nutrient source for maize cultivation in Tolon/Kumbungu District of Northern Ghana*. Tesis. Faculty of Renewable Natural Resources, Department of Agroforestry . . . .

Rezig, L., Chouaibi, M., Meddeb, W., Msaada, K., & Hamdi, S. (2019). Chemical composition and bioactive compounds of Cucurbitaceae seeds: Potential sources for new trends of plant oils. *Process Safety and Environmental Protection*, *127*, 73–81. https://doi.org/10.1016/j.psep.2019.05.005

Rolnik, A., & Olas, B. (2020). Vegetables from the Cucurbitaceae family and their products: Positive effect on human health. *Nutrition*, *78*, 110788. https://doi.org/10.1016/j.nut.2020.110788

Royani, A., Sulistiyono, E., Prasetiyo, A. B., & Subagja, R. (2018). Extraction of magnesium from calcined dolomite ore using hydrochloric acid leaching. *Proceedings of the AIP Conference*, 24–25 October 2017, Jakarta, Indonesia, AIP Publishing LLC, *1964*, 020017. https://doi.org/10.1063/1.5038299

Sabouri, Z., Sabouri, S., Moghaddas, S. S. T. H., Mostafapour, A., Gheibihayat, S. M., & Darroudi, M. (2022). Plant-based synthesis of ag-doped ZnO/MgO nanocomposites using caccinia macranthera extract and evaluation of their photocatalytic activity, cytotoxicity, and potential application as a novel sensor for detection of Pb2+ ions. *Biomass Conversion and Biorefinery*, 1–13. https://doi.org/10.1007/s13399-022-02907-1

Safford, B., Api, A., Barratt, C., Comiskey, D., Daly, E., Ellis, G., Mcnamara, C., O'Mahony, C., Robison, S., Smith, B., Thomas, R., & Tozer, S. (2015). Use of an aggregate exposure model to estimate consumer exposure to fragrance ingredients in personal care and cosmetic products. *Regulatory Toxicology and Pharmacology*, *72*(3), 673–682. https://doi.org/10.1016/j.yrtph.2015.05.017

Sawai, J., Kojima, H., Igarashi, H., Hashimoto, A., Shoji, S., Sawaki, T., Hakoda, A., Kawada, E., Kokugan, T., & Shimizu, M. (2000). Antibacterial characteristics of magnesium oxide powder. *World Journal of Microbiology and Biotechnology*, *16*(2), 187–194. https://doi.org/10.1023/A:1008916209784

Seshadri, B., Kunhikrishnan, A., Thangarajan, R., Kumpiene, J., Jinhere, P., Makino, T., Kirkham, M. B., & Sheckel, K. (2016). Redox reactions of heavy metal (loid) s in soils and sediments in relation to bioavailability and remediation. *Journal of Hazardous Materials*, *266*, 141–166. https://doi.org/10.1016/j.jhazmat.2013.12.018

Sey, E., & Belford, E. J. (2019). Levels of heavy metals and contamination status of a decommissioned tailings dam in Ghana. *EQA-International Journal of Environmental Quality*, *35*, 33–50. https://doi.org/10.6092/issn.2281-4485/9060

Seymen, M., Uslu, N., Türkmen, Ö., AL Juhaimi, F., & Özcan, M. M. (2016). Chemical compositions and mineral contents of some hull-less pumpkin seed and oils. *Journal of the American Oil Chemists' Society*, *93*(8), 1095–1099. https://doi.org/10.1007/s11746-016-2850-5

Shand, M. A. (2006). *The chemistry and technology of magnesia*. John Wiley & Sons.

Shen, Z., Hou, D., Xu, W., Zhang, J., Jin, F., Zhao, B., Pan, S., Peng, T., & Alessi, D. S. (2018). Assessing long-term stability of cadmium and lead in a soil washing residue amended with MgO-based binders using quantitative accelerated ageing. *Science of the Total Environment*, *643*, 1571–1578. https://doi.org/10.1016/j.scitotenv.2018.06.321

Shen, Z., Pan, S., Hou, D., O'Connor, D., Jin, F., Mo, L., XU, D., Zhang, Z., & Alessi, D. S. (2019). Temporal effect of MgO reactivity on the stabilization of lead contaminated soil. *Environment International*, *131*, 104990. https://doi.org/10.1016/j.envint.2019.104990

Sinkovič, L., Sinkovič, L., & Kolmanič, A. (2021). Elemental composition and nutritional characteristics of Cucurbita pepo subsp. Pepo seeds, oil cake and pumpkin oil. *Journal of Elementology*, (1/2021). https://doi.org/10.5601/jelem.2020.25.4.2072

Song, G. L., & Atrens, A. (1999). Corrosion mechanisms of magnesium alloys. *Advanced Engineering Materials*, *1*(1), 11–33. https://doi.org/10.1002/(SICI)1527-2648(199909)1:1<11:AID-ADEM11>3.0.CO;2-N

Speakman, S. A. (2014). Estimating crystallite size using XRD. *MIT Center for Materials Science and Engineering*, *2*(14), 03–08.

STEINER-ASIEDU, M., NURO-AMEYAW, P., AGBEMAFLE, I., HAMMOND, S. H., & TANO-DEBRAH, K. (2014). Nutrient composition and protein quality of four species of the Cucurbitaceae family. *Advance Journal of Food Science & Technology*, *6*(7), 843–851. https://doi.org/10.19026/ajfst.6.122

Strydom, C., Van der merwE, E., & Aphane, M. (2005). The effect of calcining conditions on the rehydration of dead burnt magnesium oxide using magnesium acetate as a hydrating agent. *Journal of Thermal Analysis and Calorimetry*, *80*(3), 659–662. https://doi.org/10.1007/s10973-005-0710-x

Tabrez, S., Khan, A. U., Hoque, M., Suhail, M., Khan, M. I., & Zughaibi, T. A. (2022). Investigating the anticancer efficacy of biogenic synthesized MgONPs: An in vitro analysis. *Frontiers in Chemistry*, *10*, 970193. https://doi.org/10.3389/fchem.2022.970193

Tang, Z.-X., & LV, B.-F. (2014). MgO nanoparticles as antibacterial agent: Preparation and activity. *Brazilian Journal of Chemical Engineering*, *31*(3), 591–601. https://doi.org/10.1590/0104-6632.20140313s00002813

THI Tran, Q. M., Thinguyen, H. A., Doan, V.-D., Tran, Q.-H., Nguyen, V. C., & Young, S.-J. (2021). Biosynthesis of zinc oxide nanoparticles using aqueous piper betle leaf extract and its application in surgical sutures. *Journal of Nanomaterials*, *2021*, 1–15. https://doi.org/10.1155/2021/8833864

Wahlström, M., Laine-Ylijoki, J., & Kaartinen, T. (2009). *Acid neutralization capacity of waste-specification of requirement stated in landfill regulations*. Nordic Council of Ministers.

WHO. (1996) . *Permissible limits of heavy metals in soil and plants*. Geneva, Switzerland.

Witte, F. (2010). The history of biodegradable magnesium implants: A review. *Acta Biomaterialia*, *6*(5), 1680–1692. https://doi.org/10.1016/j.actbio.2010.02.028

Wu, L. E., Han, F., & Liu, G. (2021). Overview of magnesium metallurgy. In *Comprehensive utilization of magnesium slag by Pidgeon process*. Springer. https://doi.org/10.1007/978-981-16-2171-0

Yusufoğlu, B., Yaman, M., & Karakuş, E. (2020). Determination of the most potent precursors of advanced glycation end products in some high-sugar containing traditional foods using high-performance liquid chromatography. *Journal of Food Processing and Preservation*, *44*(9), e14708. https://doi.org/10.1111/jfpp.14708

Zając, G., Szyszlak-Bargłowicz, J., Gołębiowski, W., & Szczepanik, M. (2018). Chemical characteristics of biomass ashes. *Energies*, *11*(11), 2885. https://doi.org/10.3390/en11112885

Zhai, P., Chen, L., HU, S., Zhang, X., Ding, D., LI, H., LI, S., Zhu, L., & YE, G. (2019). Comparison of interactions of MgO-based refractories with li-ion battery cathode materials during calcination. *International Journal of Applied Ceramic Technology*, *16*(1), 287–293. https://doi.org/10.1111/ijac.13071

Zhang, X., Zhao, W., Zhang, Y., & Jegatheesan, V. (2021). A review of resource recovery from seawater desalination brine. *Reviews in Environmental Science and Bio/technology*, *20*(2), 333–361. https://doi.org/10.1007/s11157-021-09570-4